

Particle Shape Effects on Packing Density, Stiffness, and Strength: Natural and Crushed Sands

Gye-Chun Cho¹; Jake Dodds²; and J. Carlos Santamarina³

Abstract: The size and shape of soil particles reflect the formation history of the grains. In turn, the macroscale behavior of the soil mass results from particle level interactions which are affected by particle shape. Sphericity, roundness, and smoothness characterize different scales associated with particle shape. New experimental data and results from published studies are gathered into two databases to explore the effects of particle shape on packing density and on the small-to-large strain mechanical properties of sandy soils. In agreement with previous studies, these data confirm that increased angularity or eccentricity produces an increase in e_{\max} and e_{\min} . Furthermore, the data show that increasing particle irregularity causes a decrease in stiffness yet heightened sensitivity to the state of stress; an increase in compressibility under zero-lateral strain loading; an increase in the critical state friction angle ϕ_{cs} ; and an increase in the intercept Γ of the critical state line (there is a weak effect on the slope λ). Therefore, particle shape emerges as a significant soil index property that needs to be properly characterized and documented, particularly in clean sands and gravels. The systematic assessment of particle shape will lead to a better understanding of sand behavior.

DOI: 10.1061/(ASCE)1090-0241(2006)132:5(591)

CE Database subject headings: Compression; Friction; Shape; Size; Stiffness; Strength; Particles; Sand.

Introduction

Particle size and shape reflect material composition, grain formation, and release from the mineral matrix, transportation, and depositional environments. Mechanical and chemical processes determine grain shape once it is released from the matrix (Margolis and Krinsley 1974; Rahaman 1995). The transition region from chemical to mechanical shape control occurs for a particle size between $d \sim 50$ and $400 \mu\text{m}$. Chemical action and abrasion increase with age and older sands tend to be rounder regardless of particle size. The larger the particle the higher the probability of imperfections and brittle fracturing (typically $d > 400 \mu\text{m}$). Conversely, smaller particles are stronger by lack of imperfections, then, failure by cleavage along crystal atomic planes becomes energetically advantageous and the resulting particles are more platy (Margolis and Krinsley 1974). High-coordination conditions (rather than a diametrically loaded isolated particle) promotes the splitting of elongated particles (i.e., increased cubicity) and shear abrasion.

There are three important scales in particle shape. Definitions

and their conventional evaluation in the form of dimensionless parameters follow (Fig. 1) (Wadell 1932; Krumbein 1941; Powers 1953; Krumbein and Sloss 1963; Barrett 1980):

1. Sphericity S (cf. eccentricity or platiness) refers to the global form of the particle and reflects the similarity between the particle's length, height, and width. Sphericity can be quantified as the diameter of the largest inscribed sphere relative to the diameter of the smallest circumscribed sphere.
2. Roundness R (cf. angularity) describes the scale of major surface features which are typically 1 order of magnitude smaller than the particle size. Roundness is quantified as the average radius of curvature of surface features relative to the radius of the maximum sphere that can be inscribed in the particle.
3. Smoothness (cf. roughness). Roughness describes the particle surface texture relative to the radius of the particle.

¹Associate Professor, Dept. of Civil and Environmental Engineering, Korea Advanced Institute of Science and Technology (KAIST), Daejeon 305-701, Republic of Korea (corresponding author). E-mail: gyechun@kaist.edu

²Civil Engineer, National Resources Conservation Service, Price, Utah 84501.

³Professor, School of Civil and Environmental Engineering, Georgia Institute of Technology, Atlanta, GA 30332.

Note. Discussion open until October 1, 2006. Separate discussions must be submitted for individual papers. To extend the closing date by one month, a written request must be filed with the ASCE Managing Editor. The manuscript for this paper was submitted for review and possible publication on September 9, 2004; approved on September 29, 2005. This paper is part of the *Journal of Geotechnical and Geoenvironmental Engineering*, Vol. 132, No. 5, May 1, 2006. ©ASCE, ISSN 1090-0241/2006/5-591-602/\$25.00.

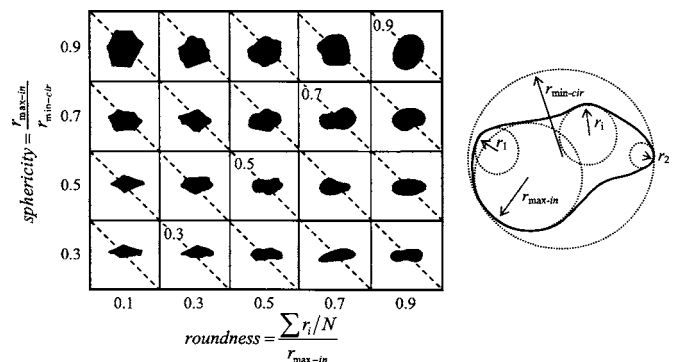


Fig. 1. Particle shape determination—sphericity S and roundness R chart. Diagonal dotted lines correspond to constant particle regularity $\rho = (R+S)/2$ (modified from Krumbein and Sloss 1963).

Table 1. Database Compiled from New Experiments (Includes Particle Shape Information)

Soil type	Gradation		Particle shape			Packing		CS parameters			K_o loading		V_s - σ relation	
	D_{50}	C_u	R	S	ρ	e_{max}	e_{min}	ϕ_{cs}^o	Γ	λ	C_c	C_s	α	β
Nevada sand	0.15	1.8	0.60	0.85	0.73	0.850	0.570	31	1.040	0.071	0.0059	0.0034	56.3	0.242
Ticino sand	0.58	1.5	0.40	0.80	0.60	0.990	0.574	37	1.050	0.053	0.0050	0.0042	70.7	0.231
Margaret river sand ^a	0.49	1.9	0.70	0.70	0.70	0.870	—	33	0.840	0.051	0.0046	0.0034	93.2	0.219
ASTM 20/30 sand	0.60	1.4	0.80	0.90	0.85	0.690	—	32	0.740	0.053	0.0038	0.0029	72.7	0.223
Ponte Vedra sand ^b	0.18	1.8	0.30	0.85	0.58	1.070	—	39	1.010	0.061	0.0052	0.0036	160.6	0.161
8M8 crushed sand	0.38	3.3	0.20	0.70	0.45	0.970	—	40	1.160	0.138	0.0220	0.0042	55.7	0.262
9C1 crushed sand	0.52	2.3	0.25	0.70	0.48	0.910	—	39	1.060	0.067	0.0050	0.0038	54.0	0.297
Jekyll Island sand ^b	0.17	1.7	0.30	0.85	0.58	1.040	—	40	0.980	0.053	—	—	139.5	0.173
ASTM graded sand	0.35	1.7	0.80	0.90	0.85	0.820	0.500	30	0.869	0.080	—	—	—	—
Blasting sand	0.71	1.9	0.30	0.55	0.43	1.025	0.698	34	1.099	0.69	—	—	—	—
Glass beads	0.32	1.4	1.00	1.00	1.00	0.720	0.542	21	0.807	0.039	—	—	—	—
Granite powder	0.09	6.2	0.40	0.24	0.32	1.296	0.482	34	1.124	0.070	—	—	—	—
Ottawa #20/30 sand	0.72	1.2	0.90	0.90	0.90	0.742	0.502	27	0.802	0.047	—	—	—	—
Ottawa F-110 sand	0.12	1.7	0.70	0.70	0.70	0.848	0.535	31	0.937	0.077	—	—	—	—
7U7-crushed sand	0.30	3.2	0.20	0.80	0.50	0.790	—	37	1.060	0.064	—	—	—	—
1K9-crushed sand	0.30	3.4	0.20	0.40	0.30	1.160	—	39	—	—	0.0160	0.0059	35.0	0.350
2Z8-crushed sand	0.48	5.0	0.10	0.60	0.35	0.860	—	41	—	—	0.0088	0.0034	25.0	0.360
5Z9-crushed sand	0.40	3.6	0.30	0.90	0.60	0.890	—	38	—	—	0.0067	0.0042	68.9	0.218
6H1-crushed sand	0.33	3.8	0.20	0.80	0.50	0.970	—	38	—	—	0.0170	0.0088	53.0	0.272
9F1-crushed sand	0.33	3.5	0.20	0.80	0.50	0.900	—	36	—	—	0.0080	0.0042	41.8	0.310
3P3-crushed sand	0.27	2.2	0.20	0.70	0.45	0.950	—	—	—	—	0.0180	0.0046	41.0	0.280
6A2-crushed sand	0.33	5.5	0.20	0.75	0.48	0.930	—	—	—	—	0.0100	0.0042	50.8	0.260
5U1-crushed sand	0.32	3.5	0.15	0.70	0.43	0.840	—	—	—	—	—	—	42.6	0.266
Sandboil sand	0.36	2.4	0.55	0.70	0.63	0.790	0.510	33	—	—	—	—	—	—
Daytona Beach sand ^c	0.23	1.4	0.62	0.70	0.66	1.000	0.640	32	—	—	—	—	—	—
Fraser River sand ^c	0.30	1.9	0.25	0.50	0.38	1.130	0.780	35	—	—	—	—	—	—
Michigan dune sand ^c	0.33	1.5	0.77	0.87	0.82	0.800	0.560	29	—	—	—	—	—	—
Ottawa #20/70 sand ^c	0.53	2.4	0.76	0.81	0.79	0.780	0.470	28	—	—	—	—	—	—
Ottawa #45 sand ^c	0.57	2.1	0.45	0.68	0.57	1.110	0.750	33	—	—	—	—	—	—
Ottawa #60/80 sand ^c	0.21	2.4	0.65	0.78	0.72	0.850	0.550	30	—	—	—	—	—	—
Ottawa # 90 sand ^c	0.27	2.2	0.40	0.60	0.50	1.100	0.730	32	—	—	—	—	—	—
Syncrude Tailings ^c	0.18	2.5	0.47	0.62	0.55	1.140	0.590	31	—	—	—	—	—	—
1O2-crushed sand	0.25	2.9	0.25	0.80	0.53	0.830	—	38	—	—	—	—	—	—
1O6-crushed sand	0.21	2.8	0.30	0.70	0.50	0.770	—	38	—	—	—	—	—	—
6F5-crushed sand	0.25	3.3	0.25	0.80	0.53	0.910	—	39	—	—	—	—	—	—
8B8-crushed sand	0.32	3.7	0.25	0.80	0.53	0.850	—	38	—	—	—	—	—	—
3C7-crushed sand	0.26	3.2	0.25	0.80	0.53	0.850	—	—	—	—	—	—	—	—
2L6-crushed sand	0.28	3.5	0.25	0.80	0.53	0.840	—	—	—	—	—	—	—	—

Note: D_{50} mean size (mm), C_u =coefficient of uniformity, R =roundness, S =sphericity, ρ =regularity= $(R+S)/2$, α =shear wave velocity (m/s) at $\sigma=1$ kPa; β =slope of V_s - σ relation; C_c =compression index; C_s =decompression index; and $\phi_{cs}, \Gamma, \lambda$ =critical state parameters.

^aIts texture is very smooth.

^bThey contain a high percentage of crushed shells (flat particles).

^cData are extracted from the study by Sukumaran and Ashmawy (2001) and Ashmawy et al. (2003).

Sphericity, roundness, and smoothness form an independent set. While sphericity and roundness increase by abrasion, they do not increase proportionally. Furthermore, chipping of a particle may increase the sphericity, but it decreases the roundness (Wadell 1932). Round particles can have nonspherical shape (e.g., elliptical particles or disk particles) and equidimensional particles can be very angular (e.g., cube or hexahedron).

The macroscale behavior of soils reflects particle level characteristics and processes. While it is intuitively recognized that particle shape affects soil behavior, a comprehensive confirmatory study is lacking (for a general review see Santamarina and Cho

2004). Furthermore, geotechnical soil classification systems—including the USCS—do not take particle shape into consideration. Therefore, the true role of particle shape on soil response remains vague.

The primary purpose of this study is to gather data with natural and crushed sands that permit investigating the role of particle shape not only on packing density (previously addressed by other researchers), but on small-to-large strain mechanical parameters as well. In addition, we explore correlations between index properties and mechanical parameters that are affected by particle shape. This study focuses on sphericity and roundness; previous

Table 2. Material Properties for Sandy Soils Compiled from Published Studies

Sand type (% fines)	Gradation		Packing		CS parameters			Test condition	References
	D_{50} (mm)	C_u	e_{max}	e_{min}	ϕ_{cs}^o	λ	Γ		
Banding 1 (0%)	0.18	1.5	0.820	0.540	32	0.020	0.850	CU	Castro et al. (1982)
Banding 5 (0%)	0.11	1.4	0.870	0.550	30	0.045	0.920	CU	Sladen et al. (1985)
Banding 6 (0%)	0.16	1.7	0.820	0.520	28.6	0.040	0.850	CU	
Banding 9 (0%)	0.14	1.6	0.800	0.530	26.8	0.030	0.850	CU	
Brenda (0%)	0.10	1.9	1.060	0.688	36	0.100	1.112	CU	Robertson et al. (1995)
Chiba (3%) ^a	0.17	2.0	1.271	0.839	34	0.085	1.265	CU	Ishihara (1993)
Chiba (18%) ^a	0.15	4.0	1.307	0.685	34	0.090	1.120	CU	
Chonan Silty (18%)	0.15	4.1	1.310	0.690	34	0.090	1.144	CU	
Dune (6%) ^a	0.21	2.3	1.080	0.590	32	0.159	1.139	CU	Konrad (1990)
Erksak 330 (0.7%)	0.33	1.8	0.753	0.527	31	0.030	0.820	CD and CU	Konrad and Watts (1995)
Fort Peck (2%) ^a	—	—	1.010	—	32	0.087	0.879	CU	Been et al. (1991)
Fraser River (0%)	0.25	1.7	1.000	0.6	34.5	0.067	1.110	CU	Chillarige et al. (1997)
Hostun RF (0%)	0.32	1.8	1.000	0.655	33.5	0.069	0.969	CU	Thevanayagam et al. (1996) Gajo and Wood (1999)
Kiyosu (0%) ^a	0.31	2.5	1.206	0.745	30	0.050	1.115	CU	Ishihara (1993)
Kogyuk 350 (0%)	0.35	1.7	0.783	0.523	31	0.014	0.784	CU	Been and Jefferies (1985)
Kogyuk 350 (2%)	0.35	1.8	0.829	0.470	31	0.065	0.845	CU	
Kogyuk 350 (5%)	0.36	2.0	0.866	0.487	31	0.105	0.925	CU	
Kogyuk 350 (10%)	0.34	2.3	0.927	0.465	31	0.175	1.056	CU	
Lagunillas (70%)	0.05	3.0	1.389	0.766	31	0.093	1.210	CU	Ishihara (1993)
Leighton Buzzard (5%)	0.12	1.8	1.023	0.665	30	0.054	1.030	CU	Been et al. (1991)
Likan (0%)	0.24	1.9	1.239	0.756	34.5	0.148	1.364	CD and CU	Lee (1995)
Lomex (0%)	0.30	2.0	1.080	0.680	35	0.050	1.100	CU	Castro et al. (1982) Sasitharan et al. (1994)
Mailiao (5%)	0.25	2.9	1.279	0.739	—	0.071	1.029	CU	Chen and Liao (1999)
Mailiao (10%)	0.22	3.5	1.151	0.595	—	0.086	0.975	CU	
Mailiao (15%)	0.21	4.2	1.031	0.440	—	0.068	0.830	CU	Chen and Liao (1999)
Massey tunnel (3%)	0.25	1.5	1.102	0.710	39.5	0.040	1.129	CU	Konrad (1997)
Monterey (0%) ^a	0.38	1.6	0.860	0.530	33	0.039	0.905	CD and CU	Riemer et al. (1990)
Monterey (16%) ^a	1.30	1.3	0.710	0.490	33	0.023	0.730	CU	Riemer and Seed (1997)
Nerlerk (0%)	0.23	1.8	0.890	0.660	30	0.030	0.885	CU	Sladen et al. (1985)
Nerlerk (2%)	0.23	2.0	0.940	0.620	30	0.040	0.880	CU	
Nevada fine (5%)	0.12	1.8	0.870	0.570	29	0.067	0.850	CU	Arulanandan et al. (1993)
Ottawa (5%)	—	—	—	—	29.5	0.067	0.809	CU	Cunning et al. (1995)
Ottawa C109 (0%)	0.35	1.7	0.820	0.500	30	0.074	0.926	CU	Sasitharan et al. (1994)
S (12%)	0.80	3.0	1.133	0.596	39	0.046	0.992	CU	Verdugo et al. (1995)
S (20%)	0.70	3.8	1.111	0.547	38	0.056	1.012	CU	
Sacramento (0%)	0.30	1.7	0.870	0.530	33.2	0.039	0.905	CU	Riemer et al. (1990) Riemer and Seed (1997)
Sand A (13%)	0.14	2.9	—	—	33.7	0.120	1.071	CU	Dobry et al. (1985)
Sand B (32%)	0.09	3.3	—	—	33.7	0.045	0.972	CU	
Sydney (0%)	0.30	1.5	0.855	0.565	31	0.073	0.969	CD and CU	Chu and Lo (1993)
Syncrude (12%)	0.17	2.4	0.930	0.550	30	0.040	0.847	CU	Sladen and Hanford (1987) Cunning et al. (1995)
Tar Island Dyke (5%) ^a	—	—	1.005	—	—	0.057	0.885	CU	Konrad and Watts (1995)
Tia Juana Silty (12%)	0.16	2.7	1.099	0.620	30.5	0.075	1.026	CU	Ishihara (1993)
Toyoura (0%)	0.17	1.7	0.977	0.597	31	0.060	1.048	CU	Ishihara (1993) Toki et al. (1986)
Toyoura (0%)	0.16	1.5	0.981	0.608	31	0.084	1.041	CU	Been et al. (1991)
Unimin 2010 (0%)	0.87	2.0	1.027	0.646	33	0.091	1.112	CU	Zhang and Garga (1997)
Well rounded (1%)	0.18	1.4	1.060	0.670	31	0.031	1.022	CU	Konrad (1990)

Note: The stress range for the critical state parameters is $p'_{cs} < \sim 400$ kPa; the CU and CD in test condition are conventional consolidated undrained and drained tests respectively.

^aCritical state parameters are based on quasisteady and steady state conditions.

studies on the effect of roughness are documented in Santamarina and Cascante (1998) and Yimsiri and Soga (1999).

Databases—Test Procedures

Two databases are compiled for this study. The first database is designed to study the effect of particle shape on soil properties (this database is summarized in Table 1—additional details can be found in Cho 2001 and Dodds 2003). Most of the data are experimentally obtained as part of this research (data from Sukumaran and Ashmawy 2001, Ashmawy et al. 2003 are included as noted). The tested soils include 17 crushed sands from Georgia (granite and carbonate) and 16 natural sands from various places around the world, and some other materials such as glass beads, granite powder, and Syncrude tailings. The measured parameters are: roundness, sphericity, grain size distribution, extreme void ratios e_{\max} and e_{\min} , small strain shear wave velocity as a measure of G_{\max} , compression and decompression indices under zero-lateral strain loading, and critical state parameters. Particle size and extreme void ratios e_{\max} and e_{\min} are obtained following standard procedures (ASTM C136, D4254, and D1557). The methodology used to obtain other parameters is presented in the following section.

The second database is compiled from published experimental results (this database is summarized in Table 2). In general, particle shape is not documented in the literature, therefore, this da-

tabase is used to complement the main database when exploring expected shape-dependent correlations between soil index properties and critical state parameters. The following soil index properties are known for this database: mean grain size D_{50} (mm), coefficient of uniformity C_u , maximum void ratio e_{\max} , minimum void ratio e_{\min} , and fines content (percentage by weight passing sieve Number 200).

Particle Shape

Sphericity and roundness can be effectively characterized by visual comparison with charts (Folk 1955; Barrett 1980). Digital image analysis facilitates the evaluation of mathematical descriptors of particle shape including Fourier analysis, fractal analysis, and other hybrid techniques (e.g., Meloy 1977; Clark 1987; Yudhbir and Abedinzadeh 1991; Kuo et al. 1996; Hyslip and Vallejo 1997; Bowman et al. 2001; Sukumaran and Ashmawy 2001). The direct measurement of roughness is cumbersome: the fractal nature of rough surfaces implies that there is no characteristic scale on the surface itself. Therefore, the relevant “observation length scale” for roughness is the interparticle contact area. Finally, shape parameters can be inferred from macroscale behavior of the soil mass. For instance, particle shape affects granular flow on inclined planes, residence time on sieves, and sedimentation time in a fluid column. However, it is not possible to separate the relative contributions of roughness, sphericity, and roundness from such individual measurements.

In this study, sphericity and roundness are determined by observing individual grains through a stereomicroscope (Leica MZ6) and comparing the observed geometry against two-dimensional (2D) figures in the chart shown in Fig. 1. Base tilting and turning grains help identify the third dimension, even when stereomicroscopy is used; the reported roundness reflects the most eccentric cross section. This procedure is repeated for 30 different grains of size $\sim D_{50}$, and average values are documented in Table 1.

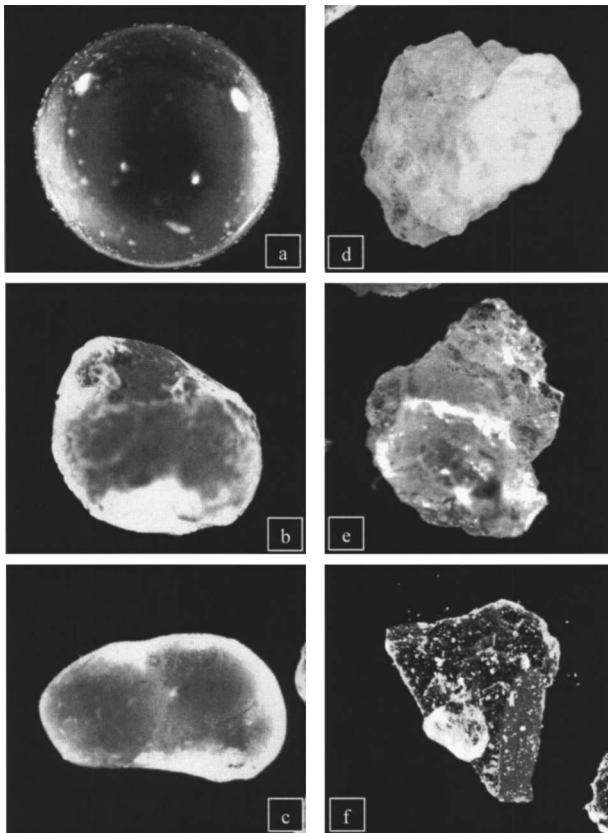


Fig. 2. Microphotographs showing various grain shapes encountered in this study: (a) glass beads $D=0.32$ mm; (b and c) ASTM 20/30 sand $D\approx 0.60$ mm; (d) Ticino sand $D=0.33$ mm; (e) crushed granite $D=0.35$ mm; and (f) fine particle from crushed granite $D\approx 0.08$ mm

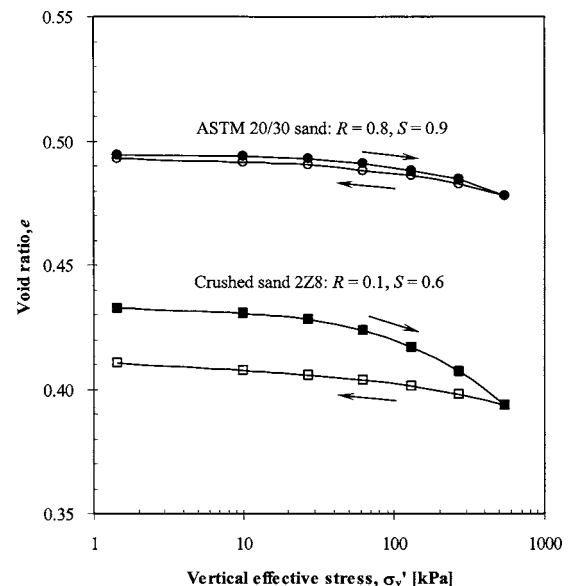


Fig. 3. Variation of void ratio with vertical effective stress during zero-lateral strain loading (additional properties for these sands can be found in Table 1)

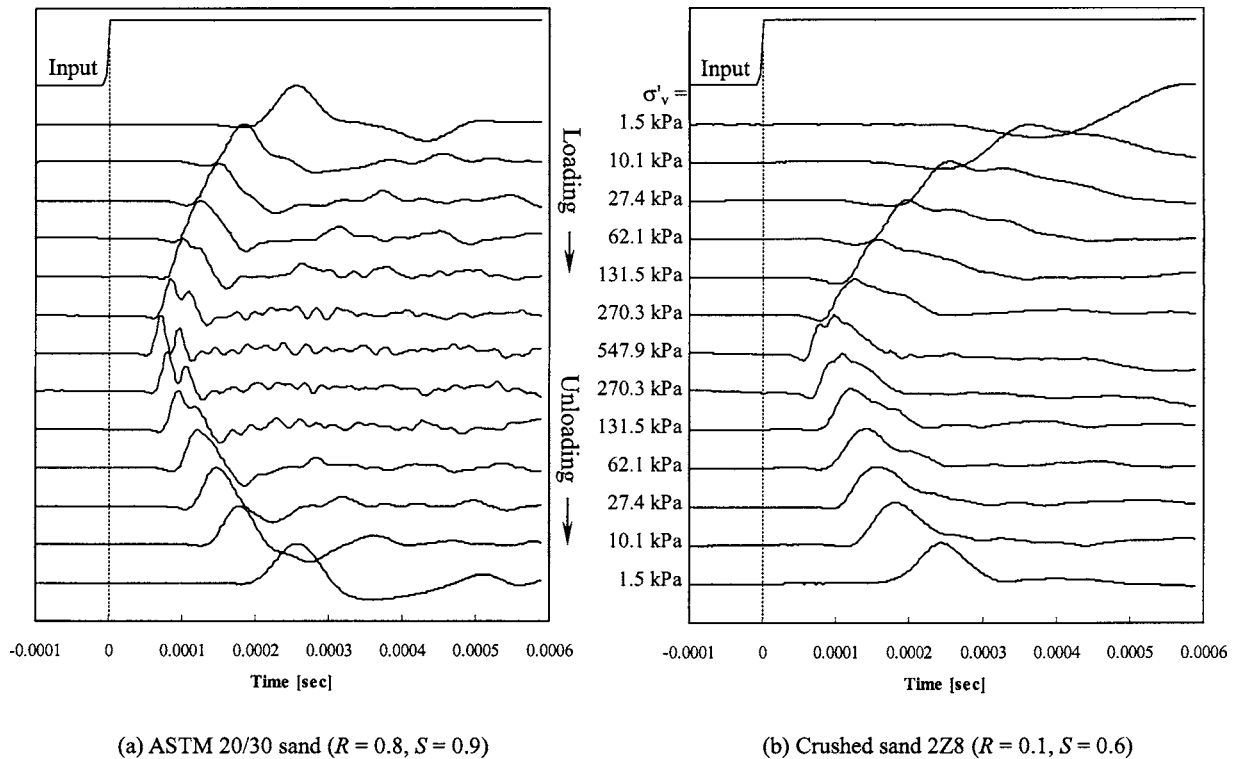


Fig. 4. Shear wave time series gathered at different vertical effective confining stresses during loading and unloading in instrumented oedometer cell (additional properties for these sands can be found in Table 1)

A handheld magnifying lens is often sufficient; therefore, the visual assessment permits the systematic determination of particle shape in standard geotechnical laboratories worldwide. Operator variability is lower than the shape variability among particles in most sands; in fact, experienced evaluators produce consistent values, and the variation in R and S is smaller than 0.1 (from a comparative study conducted with 15 students and eight different sands). Finally, the simple methodology is compatible with other expedient and meaningful procedures in geotechnical practice.

A single measure of deviation from “round spherical” shape, herein called regularity ρ , is sought to facilitate data interpreta-

tion. No a priori assumption is made with respect to the relative roles that deviations from sphericity and roundness have on macroscale soil behavior, and multiple linear combinations of R and S are explored. The expression for regularity that is most discriminatory is the average of R and S , $\rho = (R + S)/2$. Lines of constant regularity are superimposed on Fig. 1.

Microphotographs in Fig. 2 show the range of grain shapes encountered in this study. Most crushed sands exhibit similar shapes: roundness near $R = 0.2 - 0.3$ and sphericity around $S = 0.7 - 0.8$. Natural sands exhibit a wider range of shapes (typically, roundness $R = 0.3 - 0.9$ and sphericity $S = 0.5 - 0.9$). Margaret

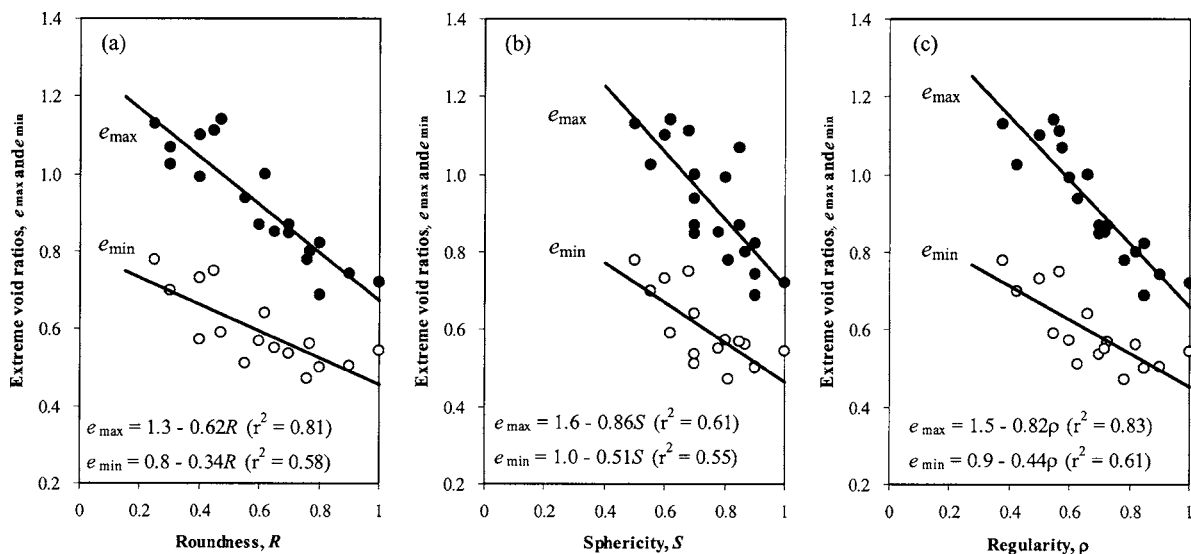


Fig. 5. Effect of particle shape on extreme void ratios (natural sands with $C_u \leq 2.5$ —data in Table 1)

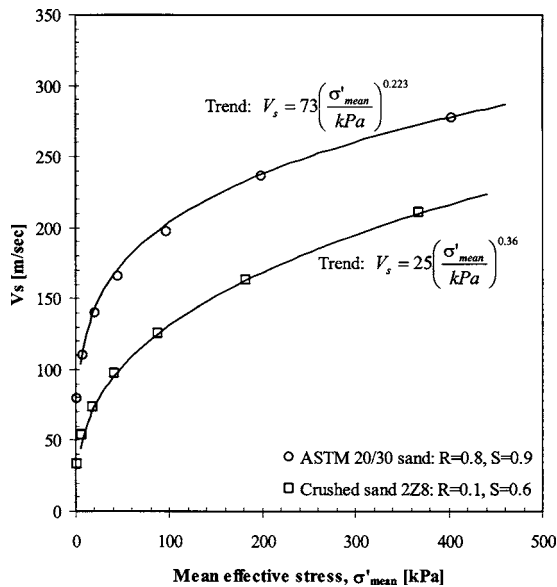


Fig. 6. Shear wave velocity versus mean effective stress on polarization plane (refer to Fig. 4—properties for these sands can be found in Table 1)

river sand has very smooth surface texture. Ponte Vedra and Jekyll Island sands contain a significant percentage of platy crushed shells. Crushed sands contain between 1 and 25% of platy mica particles. Shape varies with particle size, particularly in crushed sands: smaller particles are more planar and have sharper corners. Shape dispersion with size is minimized in this study by placing emphasis on specimens with low C_u .

Small Strain Stiffness during Zero-Lateral Strain Loading

The effect of particle shape on small strain and oedometric stiffness is studied by measuring shear wave velocity during specimen loading and unloading in an oedometric cell fitted with bender elements. Six natural sands and ten crushed sands are tested. All specimens are prepared dense by tamping each layer with a 32 mm diameter rod, starting at the outside and moving toward the center. The 100 mm diameter specimens are loaded with 2.8, 6.9, 13.7, 27.5, 55, and 110 N at 10 min intervals then unloaded in the same manner. Dial gage readings and shear wave signals are recorded prior to the next load step. Figs. 3 and 4 present typical load deformation data and received signals. The compression and decompression indices C_c and C_s are determined for the 30–300 kPa load interval for each sand (Table 1).

Critical State Parameters

Critical state captures the large-strain behavior of soils in terms of shear stress $q = (\sigma_1 - \sigma_3)$, mean effective stress $p' = (\sigma_1' + 2\sigma_3')/3$, and void ratio e . The critical state line (CSL) is the loci of critical state conditions in the $e-p'-q$ space (Roscoe et al. 1958; Schofield and Wroth 1968; Wood 1990). Its projection on the $p'-q$ space defines the strength parameter M

$$M = \frac{q_{cs}}{p'_{cs}} = \frac{6 \sin \phi_{cs}}{3 - \sin \phi_{cs}} \quad (1)$$

where the subindex CS denotes critical state. The second equality applies to axisymmetric, axial compression (e.g., triaxial test), and it is a function of the constant volume critical state friction angle ϕ_{cs} . The projection of the critical state line onto the e -log p' space defines the slope λ and intercept Γ

$$e_{cs} = \Gamma - \lambda \log \left(\frac{p'_{cs}}{1 \text{ kPa}} \right) \quad (2)$$

The determination of critical state parameters is affected by localization and limited strain level. Both difficulties are overcome in this study by subjecting homogeneous contractive specimens to drained axial loading to large strains, following the simplified procedure suggested in Santamarina and Cho (2001). Critical state parameters are corroborated for selected soils running drained triaxial tests on otherwise similar homogeneous and contractive specimens.

Results and Analyses: Shape and Soil Properties

All measured values are summarized in Table 1. The wide range of material parameters permits gaining insight into the effect of particle shape on natural and crushed sands. A comprehensive analysis of particle shape effects in different strain regimes follows.

Packing

The effect of particle shape on maximum and minimum void ratios is explored in Fig. 5. The relevance of grain size distribution on packing density is purposely removed from this figure by keeping only those soils that have $C_u \leq 2.5$ (see Youd 1973). Both e_{max} and e_{min} , and the void ratio difference $I_e = e_{max} - e_{min}$ increase as roundness and sphericity decrease. Similar observations can be found in Fraser (1935), Shimobe and Moroto (1995), Miura et al. (1998), Dyskin et al. (2001), Jia and Williams (2001), Nakata et al. (2001), and Cubrinovski and Ishihara (2002). Clearly, irregularity hinders particle mobility and their ability to attain dense packing configurations. In the extreme case of low sphericity, platy particles bridge gaps over grains and create large open voids (Guimaraes 2002).

Small Strain Behavior—Stiffness

The small-strain stiffness of a soil is measured by imposing a smaller strain than the elastic threshold strain γ_{el} (typically $\gamma_{el} < 10^{-5}$ in sands). In this range, deformations localize at interparticle contacts and the granular skeleton deforms at constant fabric. Therefore, the small-strain shear stiffness G_{max} of a soil reflects the nature of interparticle contacts, such as the Hertzian deformation of contacting smooth spherical particles. The resulting nonlinear load–deformation response determines the stress-dependent shear wave velocity (Roesler 1979; Knox et al. 1982; Lee and Stokoe 1986)

$$V_s = \alpha \left(\frac{\sigma'_{mean}}{1 \text{ kPa}} \right)^\beta = \alpha \left(\frac{\sigma'_\perp + \sigma'_\parallel}{2 \text{ kPa}} \right)^\beta \quad (3)$$

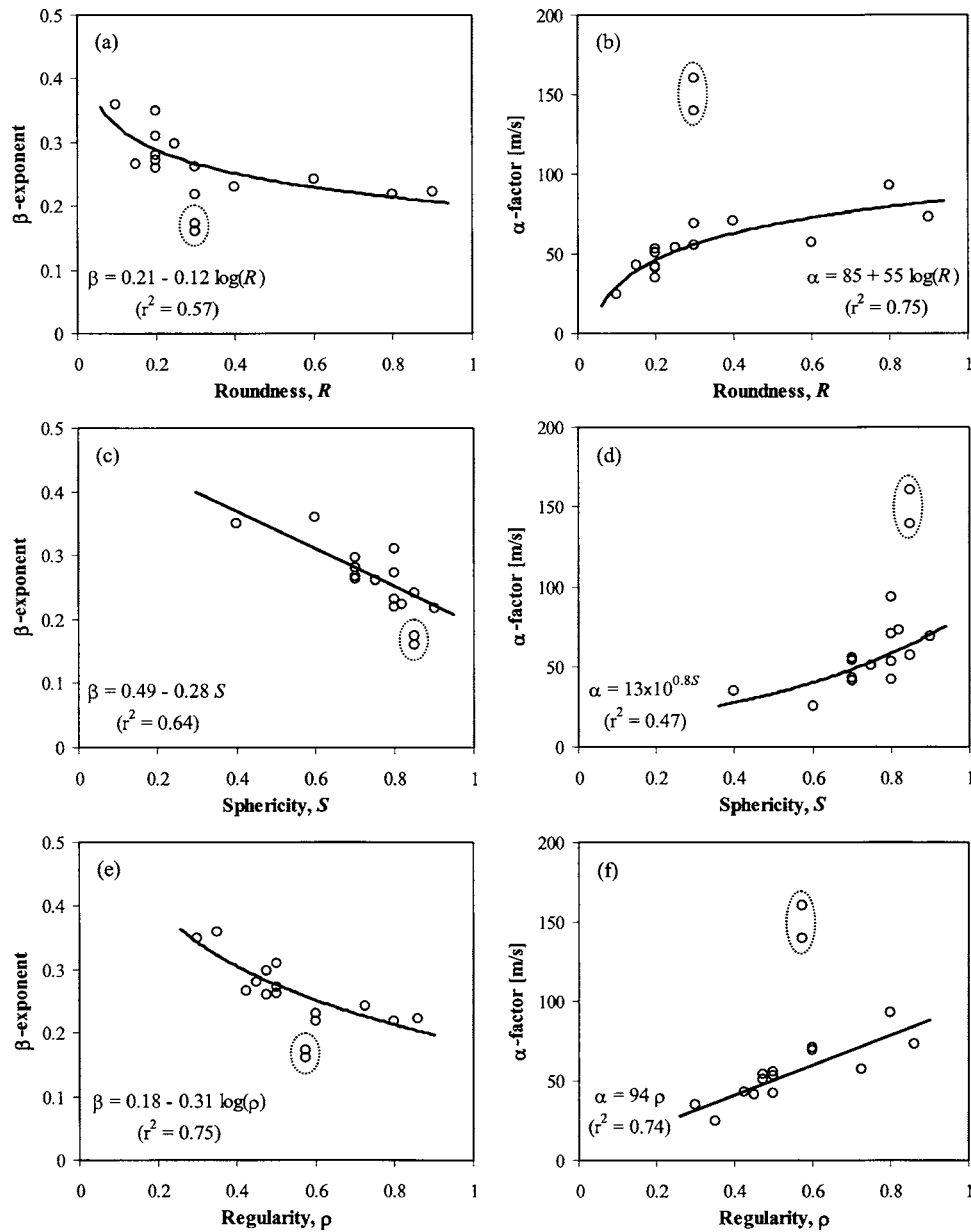


Fig. 7. Effect of particle shape on small-strain shear wave velocity (data in Table 1). Two encircled points correspond to Ponte Vedra and Jekyll Island sands which contain high percentage of crushed shells, and are not considered in trend.

where the α factor (m/s)=shear wave velocity at 1 kPa and the β exponent reflects the sensitivity of the shear wave velocity to the mean state of stress σ'_{mean} in the polarization plane (effective stresses σ'_{\perp} and σ'_{\parallel} act in the direction of particle motion and in the direction of wave propagation, respectively). Adjusted α and β parameters capture the effects of loading history and packing density. Examples of shear wave velocity variation with effective confining stress are shown in Fig. 6 (for the same two sands selected for Figs. 3 and 4). The α factor and the β exponent are obtained by fitting Eq. (3) to loading data; computed values are summarized in Table 1.

The effects of particle shape on small-strain shear wave parameters α and β are explored in Fig. 7. These results show that as sphericity, roundness, and regularity decrease, the value of α decreases while β increases. Two coexisting effects determine these trends. First, irregularity promotes looser packing (Fig. 5),

lower coordination number, and hence a softer matrix. Second, contacts between irregular particles are more deformable, as can be readily shown by comparing a cone-to-plane contact versus a sphere-to-plane contact (Goddard 1990). These two particle-level consequences of irregularity produce the observed lower stiffness (i.e., lower α) and higher sensitivity of stiffness to the state of stress (i.e., higher β). Computed α and β values satisfy the inverse relationship previously observed with a wide range of soils $\beta = 0.36 - \alpha/700$ (Santamarina et al. 2001).

The two encircled points in Fig. 7 correspond to Ponte Vedra and Jekyll Island sands which contain a high percentage of crushed shells; these two points are not considered in the trend. Similar to micaceous sands, the presence of platy particles in sands lowers the packing density, the stiffness, and the residual strength (McCarthy and Leonard 1963; de Graft-Johnson et al. 1969; Lupini et al. 1981; Hight et al. 1998; Guimaraes 2002).

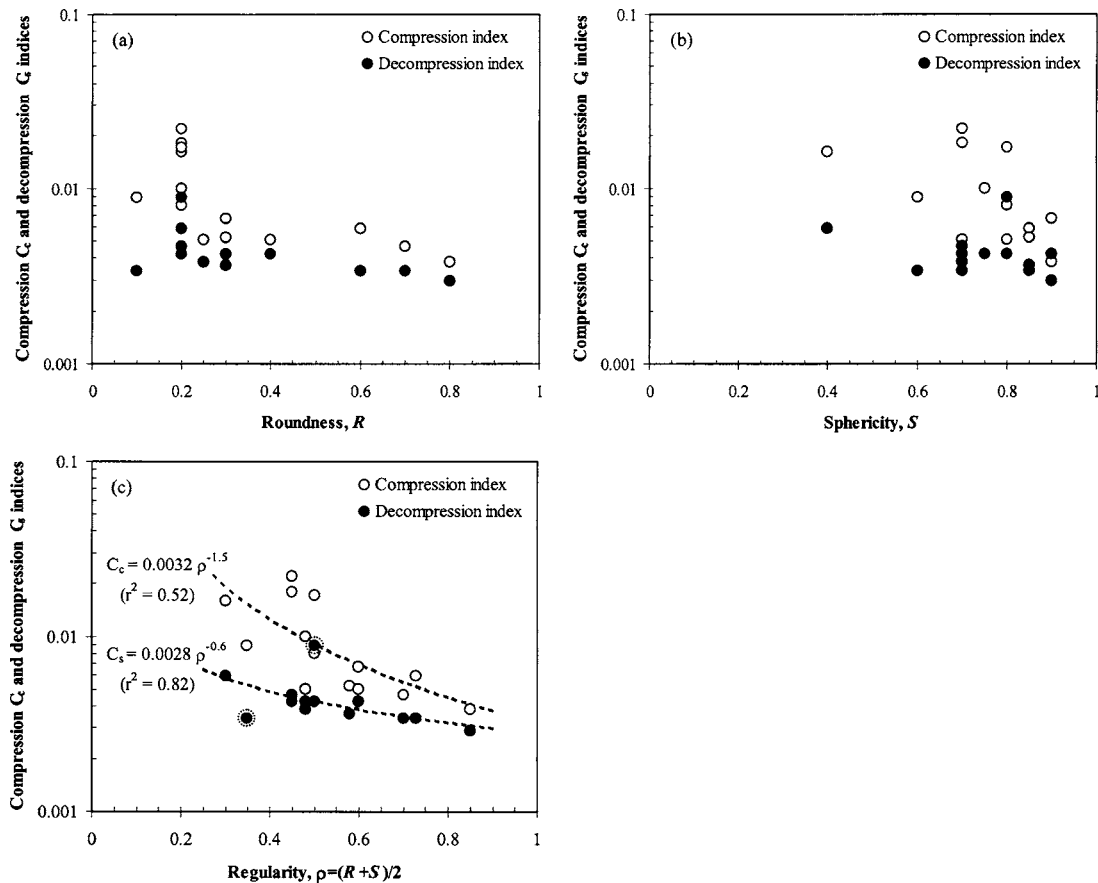


Fig. 8. Effect of particle shape on zero-lateral strain oedometric stiffness during compression and decompression (data in Table 1): (a) roundness; (b) sphericity; and (c) regularity. Correlation coefficient for decompression data excludes encircled points.

Intermediate Strain Behavior—Zero-Lateral Strain Loading

The effect of particle shape on oedometric modulus determined at zero-lateral strain is explored using the experimental data in Table 1. Fig. 8 shows that increased particle irregularity leads to higher compression and decompression indices.

Particle-level mechanisms include those discussed in previous sections, i.e., lower packing density, lower coordination number, higher contact deformation, and lower constant-fabric stiffness. In addition, new particle-scale deformation mechanisms take place in oedometric compression including: contact slippage (facilitated in smooth particles), contact breakage (intensified by angularity), and ensuing fabric changes (Coop 2005).

Large Strain Behavior—Critical State

Large strain soil behavior involves particle rotation and contact slippage. At low density, the interparticle coordination is low, shear deformation causes particle rotation and chain buckling, and the packing gradually densifies. However, rotation is hampered in dense soils with high interparticle coordination (i.e., rotational frustration), therefore, energy applied during shear loading is consumed either in dilation (to reduce coordination number) or in frictional slippage at contacts. Energy minimization dictates the interplay between these mechanisms, the statistical equilibrium at

critical state, and the evolution of anisotropy during shear. Ultimately, the shear strength of a soil reflects its ability to develop internal force and fabric anisotropy (Rothenburg and Bathurst 1989; Thornton 2000).

Within this particle-level mechanical framework, it is appropriate to hypothesize that eccentricity, angularity, and roughness add difficulty to particle rotation, enhance dilatancy, and the evolution of anisotropy, i.e., greater shear resistance. This hypothesis is tested against experimental test results summarized in Fig. 9. The three critical state parameters Γ , λ , and ϕ_{cs} decrease with increasing roundness, sphericity, and overall regularity. Roundness is more relevant to critical state friction angle ϕ_{cs} and intercept Γ than sphericity, and the following guidelines are obtained:

$$\phi_{cs} = 42 - 17R \quad (4)$$

$$\Gamma = 1.2 - 0.4R \quad (5)$$

The slope λ is poorly determined by shape parameters (the effect of particle crushing is explored in McDowell and Bolton 1998; Luzzani and Coop 2002). However, the critical state void ratio e_{cs100} at a mean principal stress $p' = 100$ kPa, which is computed

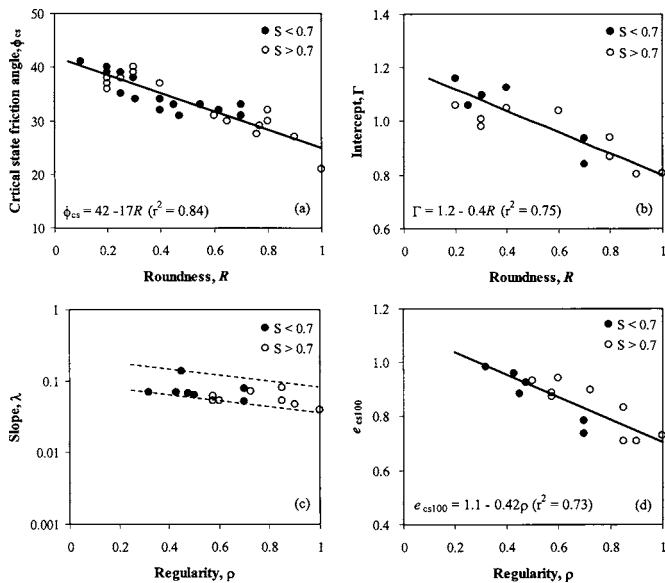


Fig. 9. Effect of particle shape on critical state parameters (data in Table 1)

as $e_{cs100} = \Gamma - 2\lambda$ [Eq. (2)], exhibits good correlation with particle regularity ρ [Fig. 9(d)]

$$e_{cs,100} = 1.1 - 0.42\rho \quad (6)$$

Clearly, the constant volume critical state friction angle ϕ_{cs} is not just dependent on mineral-to-mineral friction but strongly affected by particle shape (see also Chan and Page 1997).

Shape-Dependent Parameter Correlation

The particle shape dependency exhibited by grain packing (extreme void ratios e_{max} and e_{min}) and by mechanical parameters (V_s , C_c , C_s , Γ , λ , and ϕ_{cs}) suggests that correlations among these parameters may be justified by particle shape effects. This is investigated by combining the experimental data gathered in this study (Table 1—includes particle shape) and data gathered from the literature (Table 2—does not include particle shape).

The critical state fabric that develops at large shear strain is not expected to resemble the fabric a soil develops during e_{max} determinations by funneling, or during particle rearrangement during e_{min} measurements. However, stability conditions at the particle level are controlled by similar particle shape characteristics. Therefore, correlations between Γ (e_{cs} at $p' = 1$ kPa) and the critical state void ratio at $p' = 100$ kPa ($e_{cs100} = \Gamma - 2\lambda$) with extreme void ratios e_{max} and e_{min} are expected. Fig. 10(a and b) show that both Γ and e_{cs100} increase when extreme void ratios increase, in relation to decreased particle regularity. The intercept Γ is similar to e_{max} , and e_{cs100} corresponds to a relative density $D_r \approx 40\%$.

Weak correlations are found between the critical state friction angle ϕ_{cs} or the slope of the critical state line λ with index properties e_{max} , e_{min} , or I_e . Fig. 10(c) shows λ versus I_e and the underlying role of particle shape. By definition, the slope of the critical state line $\lambda = \Delta e_{cs} / \Delta p'_{cs}$ involves the range in possible packing densities Δe , therefore it should reflect the potential range in void ratios a soil may attain $I_e = e_{max} - e_{min}$. (Note: published critical state parameters may have been obtained from specimens that experienced localization – localization was pre-

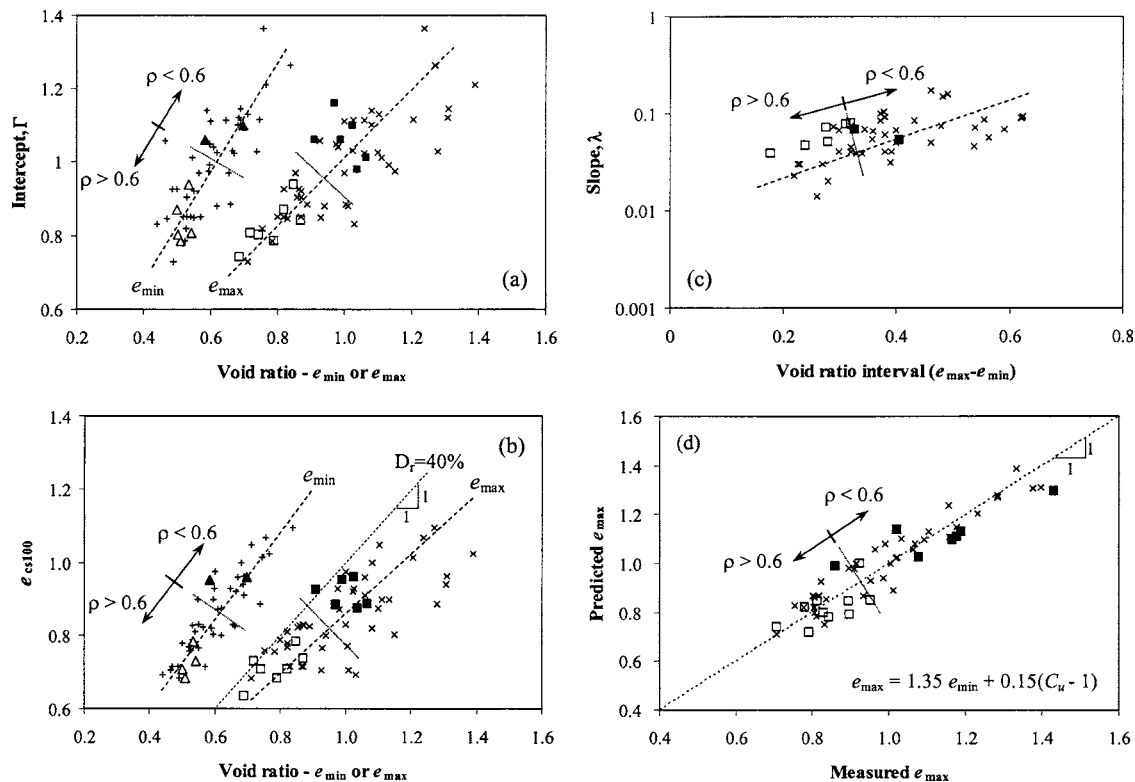


Fig. 10. Correlations between parameters (data in Tables 1 and 2). Triangular and square points are from Table 1 and particle shape information is encoded as: filled symbols represent regularity $\rho < 0.6$, empty symbols represent regularity $\rho > 0.6$. Other points (x) are (“x” is one of symbols) from Table 2.

vented in tests conducted as part of this research. While localization affects Γ and λ , it has virtually no effect on ϕ_{cs} —Santamarina and Cho 2004).

Fig. 10(d) presents measured values of e_{max} versus the predicted values computed from e_{min} taking into consideration the coefficient of uniformity C_u . Soils with known particle shape are distinguished according to regularity. This plot captures the interplay between the coefficient of uniformity and particle shape on grain packing (Youd 1973).

Conclusions and Recommendations

The size and shape of soil particles reflect the formation history of the grains. Chemical processes determine the size and shape of clays and silts, while mechanical processes prevail in sands and gravels. Most manufactured crushed sands exhibit similar shapes (roundness near $R=0.2-0.3$ and sphericity around $S=0.7-0.8$). Natural sands have a wider range of shapes (typical roundness $R=0.3-0.9$ and sphericity $S=0.5-0.9$).

Particle shape characteristics manifest at various scales: the global form at the scale of the particle, angularity at the scale of major surface features, and roughness at the scale of surface texture. Each scale reflects aspects of the formation history, and participates in determining the global behavior of the soil mass. The decrease in particle regularity (decrease sphericity and/or roundness) leads to:

1. Increase in extreme void ratios e_{max} and e_{min} , and void ratio interval $I_e=e_{max}-e_{min}$ (as observed in previous studies);
2. Decrease in small-strain stiffness (α coefficient), yet increased sensitivity to the state of stress (β exponent);
3. Increase in the compressibility under zero-lateral strain loading (C_c);
4. Increase in the constant volume critical state friction angle ϕ_{cs} ; and
5. Increase in the critical state line intercept Γ , and a weak effect on the slope λ of the critical state line (void-stress space).

Although the fabric at critical state is not expected to resemble the fabric at e_{max} and e_{min} , stability conditions at the particle level are controlled by similar particle characteristics. Therefore, Γ , e_{cs100} , e_{max} , and e_{min} increase as particle regularity decreases. Furthermore, the value Γ of the critical state line at $p'=1$ kPa is similar to e_{max} , and the void ratio e_{cs100} on the critical state line at $p'=100$ kPa corresponds to a relative density $D_r \approx 40\%$.

Several particle-level mechanisms associated with particle irregularity are responsible for the observed macroscale response, including: hindered rotation, slippage and ability for particle rearrangement; lower interparticle coordination; increased particle-level dilation; lower contact stiffness; and higher proneness to contact damage. (Note: the effect of grain size distribution was minimized by data grouping before processing the data; still, some influence of C_u should be expected in observed trends.)

The relevance of grain size and grain size distribution in soil behavior is extensively recognized in soil classification systems, such as the USCS. While particle shape is overlooked in current classification guidelines, it emerges as a determining parameter in soil behavior. It is recommended that particle shape be assessed and explicitly documented as part of every soil characterization exercise, in particular when clean sands or gravels are involved.

Acknowledgments

Support was provided by NSF (Project: The Effect of Internal Scales in Soil Behavior), the Georgia Mining Industry, The Goizueta Foundation, and the Smart Infra-Structure Technology Center (SISTeC) under KOSEF. The writers are grateful to the reviewers for their detailed comments.

References

- Arulanandan, K., Seed, H. B., Yogachandran, C., Muraleetharan, K. K., and Seed, R. B. (1993). "Centrifuge study on volume changes and dynamic stability of earth dams." *J. Geotech. Eng.*, 119(11), 1717–1731.
- Ashmawy, A. K., Sukumaran, B., and Vinh Hoang, V. (2003). "Evaluating the influence of particle shape on liquefaction behavior using discrete element modelling." *Proc. 13th Int. Offshore and Polar Engineering Conf.*, ISOPE, Honolulu, Vol. 2, 542–549.
- Barrett, P. J. (1980). "The shape of rock particles, a critical review." *Sedimentology*, 27, 291–303.
- Been, K., and Jefferies, M. G. (1985). "A state parameter for sands." *Geotechnique*, 35(2), 99–112.
- Been, K., Jefferies, M. G., and Hachey, J. (1991). "The critical state of sands." *Geotechnique*, 41(3), 365–381.
- Bowman, E. T., Soga, K., and Drummond, W. (2001). "Particle shape characterization using Fourier descriptor analysis." *Geotechnique*, 51(6), 545–554.
- Castro, G., Enos, J. L., France, J. W., and Poulos, S. J. (1982). "Liquefaction induced by cyclic loading." *Rep. No. NSF/CEE-82018*, National Science Foundation, Washington, D.C.
- Chan, L. C. Y., and Page, N. W. (1997). "Particle fractal and load effects on internal friction in powders." *Powder Technol.*, 90, 259–266.
- Chen, Y. C., and Liao, T. S. (1999). "Studies of the state parameter and liquefaction resistance of sands." *Earthquake Geotechnical Engineering: Proc., 2nd Int. Conf.*, Lisbon, Portugal, P. S. Seco e Pinto, ed., A.A. Balkema, Rotterdam, The Netherlands, 513–518.
- Chillarige, A. V., Robertson, P. K., Morgenstern, N. R., and Christian, H. A. (1997). "Evaluation of the in situ state of Fraser River sand." *Can. Geotech. J.*, 34(4), 510–519.
- Cho, G. C. (2001). "Unsaturated soil stiffness and post-liquefaction shear strength." Ph.D. thesis, Georgia Institute of Technology, Atlanta.
- Chu, J., and Lo, S. C. R. (1993). "On the measurement of critical state parameters of dense granular soils." *Geotech. Test. J.*, 16(1), 27–35.
- Clark, N. N. (1987). "A new scheme for particle shape characterization based on fractal harmonics and fractal dimensions." *Powder Technol.*, 51, 243–249.
- Coop, M. R. (2005). "On the mechanics of reconstituted and natural sands." *Proc., 3rd Int. Symp. on Deformation Characteristics of Geomaterials*, Lyon, France, H. Di Benedetto, T. Doanh, H. Geoffroy, and C. Sauzeat, eds., A.A. Balkema, Rotterdam, The Netherlands, 29–58.
- Cubrinovski, M., and Ishihara, K. (2002). "Maximum and minimum void ratio characteristics of sands." *Soils Found.*, 42(6), 65–78.
- Cunning, J. C., Robertson, P. K., and Sego, D. C. (1995). "Shear wave velocity to evaluate in situ state of cohesionless soils." *Can. Geotech. J.*, 32, 848–858.
- de Graft-Johnson, J. W. S., Bhatia, H. S., and Gidigas, D. M. (1969). "The strength characteristics of residual micaceous soils and their application to stability problems." *Proc. 7th Int. Conf. on Soil Mechanics and Foundation Engineering*, Mexico, 165–172.
- Dobry, R., Vasquez-Herrera, A., Mohamad, R., and Vucetic, M. (1985). "Liquefaction flow failure of silty sand by torsional cyclic tests." *Advances in the Art of Testing Soils under Cyclic Conditions, Proc. of a Session Sponsored by the Geotechnical Engineering Division in Conjunction with the ASCE Convention*, Detroit, V. Khosla, ed., 29–50.
- Dodds, J. S. (2003). "Particle shape and stiffness—Effects on soil behavior." M.Sc. thesis, Georgia Institute of Technology, Atlanta.

- Dyskin, A. V., Estrin, Y., Kanel-Belov, A. J., and Pasternak, E. (2001). "Toughening by fragmentation—How topology helps." *Adv. Eng. Mater.*, 3(1), 885–888.
- Folk, R. L. (1955). "Student operator error in determination of roundness, sphericity, and grain size." *J. Sediment. Petrol.*, 25(4), 297–301.
- Fraser, H. J. (1935). "Experimental study of the porosity and permeability of elastic sediments." *J. Geol.*, 13(8), 910–1010.
- Gajo, A., and Wood, M. (1999). "A kinematic hardening constitutive model for sands: The multiaxial formulation." *Int. J. Numer. Analyt. Meth. Geomech.*, 23, 925–965.
- Goddard, J. D. (1990). "Nonlinear elasticity and pressure-dependent wave speeds in granular media." *Proc. R. Soc. London, Ser. A* 430, 105–131.
- Guimaraes, M. (2002). "Crushed stone fines and ion removal from clay slurries—Fundamental studies." Ph.D. thesis, Georgia Institute of Technology, Atlanta.
- Hight, D. W., Georgiannou, V. N., Martin, P. L., and Mundegar, A. K. (1998). "Flow slides in micaceous sand." *Problematic soils*, E. Yanagisawa, N. Moroto, and T. Mitachi, eds., Sendai, Japan, 945–958.
- Hyslip, J. P., and Vallejo, L. E. (1997). "Fractal analysis of the roughness and size distribution of granular materials." *Eng. Geol. (Amsterdam)*, 48, 231–244.
- Ishihara, K. (1993). "The Rankine Lecture: Liquefaction and flow failure during earthquakes." *Geotechnique*, 43(3), 351–415.
- Jia, X., and Williams, R. A. (2001). "A packing algorithm for particles of arbitrary shapes." *Powder Technol.*, 120, 175–186.
- Knox, D. P., Stokoe, K. H., and Kopperman, S. E. (1982). "Effect of state of stress on velocity of low-amplitude shear waves propagating along principal stress directions in dry sand." *Rep. No. GR82-23*, Civil Engineering Dept., Univ. of Texas, Austin, Tex.
- Konrad, J. M. (1990). "Minimum undrained strength versus steady-state strength of sands." *J. Geotech. Eng.*, 116(6), 948–963.
- Konrad, J. M. (1997). "In situ sand state from CPT: Evaluation of a unified approach at two CANLEX sites." *Can. Geotech. J.*, 34(1), 120–130.
- Konrad, J. M., and Watts, B. D. (1995). "Undrained shear strength for liquefaction flow failure analysis." *Can. Geotech. J.*, 32, 783–794.
- Krumbein, W. C. (1941). "Measurement and geological significance of shape and roundness of sedimentary particles." *J. Sediment. Petrol.*, 11(2), 64–72.
- Krumbein, W. C., and Sloss, L. L. (1963). *Stratigraphy and sedimentation*, 2nd Ed., Freeman and Company, San Francisco.
- Kuo, C.-Y., Frost, J. D., Lai, J. S., and Wang, L. B. (1996). "Three-dimensional image analysis of aggregate particle from orthogonal projections." *Transp. Res. Rec.*, Transportation Research Board, Washington, D.C., 1526, 98–103.
- Lee, C. J. (1995). "Static shear and liquefaction potential of sand." *Proc., 3rd Int. Conf. on Recent Advances in Geotechnical Earthquake Engineering and Soil Dynamics*, St. Louis, Vol. 1, 115–118.
- Lee, S. H. H., and Stokoe, K. H. (1986). "Investigation of low-amplitude shear wave velocity in anisotropic material." *Rep. No. GR86-06*, Civil Engineering Dept., Univ. of Texas, Austin, Tex.
- Lupini, J. F., Skinner, A. E., and Vaughan, P. R. (1981). "The drained residual strength of cohesive soils." *Geotechnique*, 31(2), 181–213.
- Luzzani, L., and Coop, M. R. (2002). "On the relationship between particle breakage and the critical state of sands." *Soils Found.*, 42(2), 71–82.
- Margolis, S. V., and Krinsley, D. H. (1974). "Processes of formation and environmental occurrence of microfeatures on detrital quartz grains." *Am. J. Sci.*, 274, 449–464.
- McCarthy, D. F., and Leonard, R. J. (1963). "Compaction and compression characteristics of micaceous fine sands and silts." *Highw. Res. Rec.*, 22, 23–37.
- McDowell, G. R., and Bolton, M. D. (1998). "On the micromechanics of crushable aggregates." *Geotechnique*, 48(5), 667–679.
- Meloy, T. P. (1977). "Fast Fourier transforms applied to shape analysis of particle silhouettes to obtain morphological data." *Powder Technol.*, 17, 27–35.
- Miura, K., Maeda, K., Furukawa, M., and Toki, S. (1998). "Mechanical characteristics of sands with different primary properties." *Soils Found.*, 38, 159–172.
- Nakata, Y., Kato, Y., Hyodo, M., Hyde, A. F. L., and Murata, H. (2001). "One-dimensional compression behaviour of uniformly graded sand related to single particle crushing strength." *Soils Found.*, 41(2), 39–51.
- Powers, M. C. (1953). "A new roundness scale for sedimentary particles." *J. Sediment. Petrol.*, 23(2), 117–119.
- Rahaman, M. N. (1995). *Ceramic processing and sintering*, Dekker, New York.
- Riemer, M. F., and Seed, R. B. (1997). "Factors affecting apparent position of steady-state line." *J. Geotech. Geoenviron. Eng.*, 123(3), 281–288.
- Riemer, M. F., Seed, R. B., Nicholson, P. G., and Jong, H. L. (1990). "Steady state testing of loose sands: limiting minimum density." *J. Geotech. Eng.*, 116(2), 332–337.
- Robertson, P. K., Sasitharan, S., Cunnings, J. C., and Segoo, D. C. (1995). "Shear-wave velocity to evaluate in-situ state of Ottawa sand." *J. Geotech. Eng.*, 121(3), 262–273.
- Roesler, S. K. (1979). "Anisotropic shear modulus due to stress anisotropy." *J. Geotech. Eng. Div., Am. Soc. Civ. Eng.*, 105, 871–880.
- Roscoe, K. H., Schofield, A. N., and Wroth, C. P. (1958). "On the yielding of soils." *Geotechnique*, 8, 22–53.
- Rothenburg, L., and Bathurst, R. J. (1989). "Analytical study of induced anisotropy in idealized granular material." *Geotechnique*, 49, 601–614.
- Santamarina, J. C., and Cascante, G. (1998). "Effect of surface roughness on wave propagation parameters." *Geotechnique*, 48(1), 129–137.
- Santamarina, J. C., and Cho, G. C. (2001). "Determination of critical state parameters in sandy soils-simple procedure." *Geotech. Test. J.*, 24(2), 185–192.
- Santamarina, J. C., and Cho, G. C. (2004). "Soil behaviour: The role of particle shape." *Advances in geotechnical engineering: The Skempton Conference*, R. J. Jardine, D. M. Potts, and K. G. Higgins, eds., Vol. 1, Thomas Telford, London, 604–617.
- Santamarina, J. C., Klein, K. A., and Fam, M. A. (2001). *Soils and waves—Particulate materials behavior, characterization and process monitoring*, Wiley, New York.
- Sasitharan, S., Robertson, P. K., Segoo, D. C., and Morgenstern, N. R. (1994). "State-boundary surface for very loose sand and its practical implications." *Can. Geotech. J.*, 31, 321–334.
- Schofield, A. N., and Wroth, P. (1968). *Critical state soil mechanics*, McGraw-Hill, New York.
- Shimobe, S., and Moroto, N. (1995). "A new classification chart for sand liquefaction." *Earthquake geotechnical engineering*, K. Ishihara, ed., Balkema, Rotterdam, The Netherlands, 315–320.
- Sladen, J. A., D'Hollander, R. D., and Krahn, J. (1985). "The liquefaction of sands, a collapse surface approach." *Can. Geotech. J.*, 22, 564–578.
- Sladen, J. A., and Handford, G. (1987). "A potential systematic error in laboratory testing of very loose sand." *Can. Geotech. J.*, 24, 462–466.
- Sukumaran, B., and Ashmawy, A. K. (2001). "Quantitative characterization of the geometry of discrete particles." *Geotechnique*, 51(7), 171–179.
- Thevanayagam, S., Wang, C. C., and Ravishankar, K. (1996). "Determination of post-liquefaction strength: steady state vs residual strength." *Uncertainty in the geological environment: From Theory to practice, Proc., uncertainty '96*, Schackelford et al., eds., *Geotechnical Special Publication No. 58*, Vol. 2, 1210–1224.
- Thornton, C. (2000). "Numerical simulations of deviatoric shear deformation of granular media." *Geotechnique*, 50(1), 43–53.
- Toki, S., Tatsuoka, F., Miura, S., Yoshimi, Y., Yasuda, S., and Makihara, Y. (1986). "Cyclic undrained triaxial strength of sand by a cooperative test program." *Soils Found.*, 26(3), 117–128.
- Verdugo, R., Castillo, P., and Briceno, L. (1995). "Initial soil structure and steady-state strength." *Proc., 1st Int. Conf. on Earthquake Geotechnical Engineering*, K. Ishihara, ed., Vol. 1, Balkema, Rotterdam,

- The Netherlands, 209–214.
- Wadell, H. (1932). “Volume, shape, and roundness of rock particles.” *J. Geol.*, 40, 443–451.
- Wood, D. M. (1990). *Soil behavior and critical state soil mechanics*, Cambridge University Press, Cambridge, U.K.
- Yimsiri, S., and Soga, K. (1999). “Effect of surface roughness on small-strain modulus: micromechanics view.” *Proc., 2nd Int. Symp. on Pre-failure Deformation Characteristics of Geomaterials*, M. Jamiolkowski et al., eds., Torino, Italy, 597–602.
- Youd, T. L. (1973). “Factors controlling maximum and minimum densities of sands.” *ASTM Spec. Tech. Publ.*, 523, 98–112.
- Yudhbir, , and Abedinzadeh, R. (1991). “Quantification of particle shape and angularity using the image analyzer.” *Geotech. Test. J.*, 14(3), 296–308.
- Zhang, H., and Garga, V. K. (1997). “Quasi-steady state: A real behaviour?” *Can. Geotech. J.*, 34, 749–761.